MICROSCOPY RESEARCH AND TECHNIQUE 38:315–328 (1997)

Spray-Freezing Freeze Substitution (SFFS) of Cell Suspensions for Improved Preservation of Ultrastructure

STEPHEN D. FIELDS,[1,2] GREGORY W. STROUT,[1] AND SCOTT D. RUSSELL[1,2]*
[1]*Samuel Roberts Noble Electron Microscopy Laboratory, University of Oklahoma, Norman, Oklahoma 73019*
[2]*Department of Botany and Microbiology, University of Oklahoma, Norman, Oklahoma 73019*

KEY WORDS Chroomonas; Dictyostelium; Gymnodinium; Procholorococcus; ultrarapid-freezing

ABSTRACT Some unicellular organisms present challenges to chemical fixations that lead to common, yet obvious, artifacts. These can be avoided in entirety by adapting spray-freezing technology to ultrarapidly freeze specimens for freeze substitution. To freeze specimens, concentrated suspensions of cells ranging in diameter from 0.5–30 µm were sprayed with an airbrush at 140–200 kPa (1.05–1.5 torr; 20.3–29.0 psi) into a nylon mesh transfer basket submerged in liquid propane. After freezing, the mesh basket containing the frozen sample was lifted out of the chamber, drained and transferred through several anhydrous acetone rinses at 188 K (−85°C). Freeze substitution was conducted in 1% tannic acid/1% anhydrous glutaraldehyde in acetone at 188 K (−85°C), followed by 1% OsO_4/acetone at 277 K (4°C). Freeze substitution was facilitated using a shaking table to provide gentle mixing of the substitution medium on dry ice. High quality freezing was observed in 70% of spray-frozen dinoflagellate cells and in 95% of spray-frozen cyanobacterial cells. These could be infiltrated and observed directly; however, overall ultrastructural appearance and membrane contrast were improved when the freeze-substituted cells were rehydrated and post-fixed in aqueous OsO_4, then dehydrated and embedded in either Spurr's or Epon resin. Ultrastructural preservation using this ultrarapid freezing method provided specimens that were consistently superior to those obtainable in even the best comparable chemical fixations. *Microsc. Res. Tech. 38:315–328, 1997.*

INTRODUCTION

The primary goal of fixation in biological electron microscopy is to preserve and stabilize cellular constituents in a natural state. Chemical fixatives often fall short of this objective because artifacts may be introduced as a result of slow penetration of fixatives (Mersey and McCully, 1978), retention of osmotic activity by chemically-fixed membranes (Bowers and Maser, 1988; Lee et al., 1982), and continued activity of metabolic processes after the introduction of the fixative solution (Kellenberger et al., 1992). In contrast, ultrarapid freezing may yield superior ultrastructural preservation because cellular constituents are immobilized in crystal-free, vitreous ice in milliseconds (Gilkey and Staehelin, 1986; Knoll et al., 1987; Quintana, 1994). Successful cryofixation depends on achieving ultrarapid cooling rates above 10^4 C sec^{-1} (see Dubochet et al., 1982; Mayer and Brüggeller, 1982). At slower freezing rates, ice crystals nucleate and propagate within cells, causing damage such as membrane disruptions and redistribution of cytoplasmic solutes that are easily observed using transmission electron microscopy (TEM). Cooling rates are strongly influenced by such factors as the freezing method, specimen geometry and water content of the sample.

Although a variety of freezing devices are capable of achieving ultrarapid rates of cooling (for reviews see Gilkey and Staehelin, 1986; Menco, 1986; Plattner and Bachmann, 1982; Plattner and Knoll, 1984; Ryan, 1992; Ryan and Knoll, 1994), many are not suitable for freezing cell suspensions because their designs are optimized for processing tissue samples, or because they cannot efficiently freeze the large amount of water associated with cell suspensions. One solution is to freeze samples in thin films in order to reduce the water volume of cell suspensions (e.g., Hyde et al., 1991; Lancelle et al., 1986; Lokhorst and Segaar, 1989; Murray and Ward, 1987; Ridge, 1990), but the proportion of cells with high quality preservation may be as low as 10% under optimal conditions (Ridge, 1990). Cryoprotectants such as glycerol have also been used to reduce ice crystal growth, but these are often toxic to living cells or may cause cell alterations that include swelling, disruption of the plasma membrane and/or vesiculation of endomembrane systems prior to freezing (Plattner et al., 1972; 1973; Skaer, 1981).

One method that seems theoretically ideal for ultrarapid freezing of cell suspensions is that of spray-freezing, but it has received little practical attention for routine TEM. The basis of spray-freezing is to achieve atomization of a cell suspension by passing it through a

Contract grant sponsor: National Science Foundation; contract grant number: DEB-9311481; contract grant sponsor: U.S. Department of Agriculture; contract grant numbers: 91-37304-6471 and 95-37304-2361.

Stephen D. Fields' current address is Program in Molecular and Cell Biology, Oklahoma Medical Research Foundation, 825 N.E. 13th Street, Oklahoma City, OK 73104.

*Correspondence to: Dr. Scott D. Russell, Department of Botany and Microbiology, University of Oklahoma, Norman, OK 73019. E-mail: srussell@ou.edu

Accepted in revised form 23 March 1997

TABLE 1. Investigations applying spray- or specimen jet-freezing to the study of organelles and whole cells[1]

Reference	Technique	Specimen
Bachmann et al (1972)	FF, FE	*Chlorella*
Bittermann et al. (1992)	FS (SJF)	*Paramecium*
Geanacopoulos and Gear (1988)	FF, FE	Blood platelets
Horowitz et al. (1990)	FS	Nuclei
Knoll et al. (1991)	FF, FS (SJF)	*Paramecium*
Lang and Bronk (1978)	FF, FE	Mitochondria
Lang et al. (1976)	FF, FE	Mitochondria
Linder and Staehelin (1979)	FS	*Leptomonas*
Miller and Dahl (1982)	FF	Liposomes
Pfaller and Rovan (1978)	FD, FE	Spermatozoa
Pfaller et al. (1976)	FD, FE	Spermatozoa
Plattner (1971)	FE	Spermatozoa
Plattner et al. (1972)	FF, FE	*Chlorella, Euglena,* spermatozoa
Plattner et al. (1973)	FF, FE	*Aerobacter, Chlorella, Euglena, Paramecium, Selenastrum,* spermatozoa
Rand et al. (1985)	FF	Vesicle fusion
Williams (1953)	FD	TMV, red blood cells

[1]FD, freeze drying; FE, freeze etching; FF, freeze fracture; FS, freeze substitution; SJF, specimen jet freezing.

narrow aperture at low pressure and freezing the droplets in a suitable cryogen. A variation of spray-freezing is specimen jet-freezing, where cell suspensions are introduced as slender streams of fluid into the cryogen (Bitterman et al., 1992; Mayer and Brüggeller, 1982; Knoll et al., 1991). Ultrarapid rates of cooling may be achieved in a large proportion of cells using spray-freezing because: (1) the spherical shape of the microdroplet, if kept below 100 µm, is ideal for omnidirectional heat removal (Moor, 1973), and (2) the speed of entry into the cryogen is sufficient to provide ultrarapid rates of heat removal. Although spray-freezing was first used in combination with freeze-drying (Williams, 1953), most spray-freezing devices have been optimized for freeze fracture and freeze etching, with surprisingly few adaptations for routine freeze substitution (Table 1).

In working with various cell suspensions, we developed a spray-freezing technique that addresses many of the difficulties associated with freeze substitution, including cryogen disposal, complete removal of large volumes of water at low temperatures, and transfer of samples between substitution media. To demonstrate the suitability of this technique, spray-freezing, followed by freeze substitution, was applied to the freshwater dinoflagellate, *Gymnodinium acidotum,* the free-living marine prochlorophyte, *Prochlorococcus marinus* (Chisholm et al., 1988, 1992), a photosynthetic cryptomonad, *Chroomonas coerulea,* and the amoebae of the slime mold, *Dictyostelium discoideum*. In conjunction with the spray-freezer, a freeze substitution protocol that improves visualization of membranes was also developed that combines the better structural preservation of ultrarapidly fixed specimens with the advantages of aqueous staining. In light of the improved fixation, some of the ultrastructural features of chemically-fixed *G. acidotum* need to be re-examined.

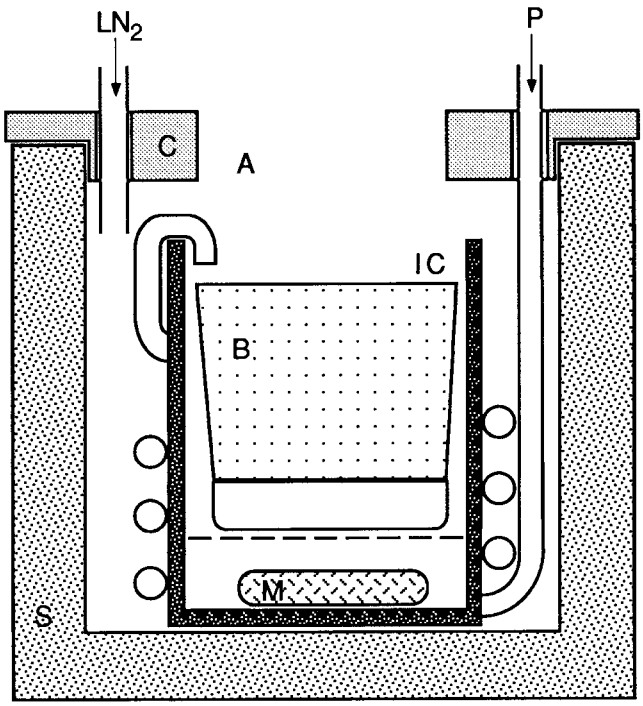

Fig. 1. The cryogenic chamber is cooled by introducing liquid nitrogen into the Styrofoam cooling chamber via a funnel inserted through a hole in the removable Plexiglass cover. Propane from a commercial tank is condensed in copper coils (arrowheads) submerged in the liquid nitrogen and collected in the inner cryochamber. The chamber can be placed on a magnetic stir plate in order to drive a stir bar to prevent propane from freezing too rapidly. Specimen droplets are sprayed from an airbrush through the central aperture in the cover and collected in the mesh basket submerged in the liquid propane. A, central aperture; B, mesh collecting basket; C, Plexiglas cover; IC, inner cryochamber; LN_2, liquid nitrogen; M, magnetic stir bar; P, propane; S, Styrofoam cooling chamber.

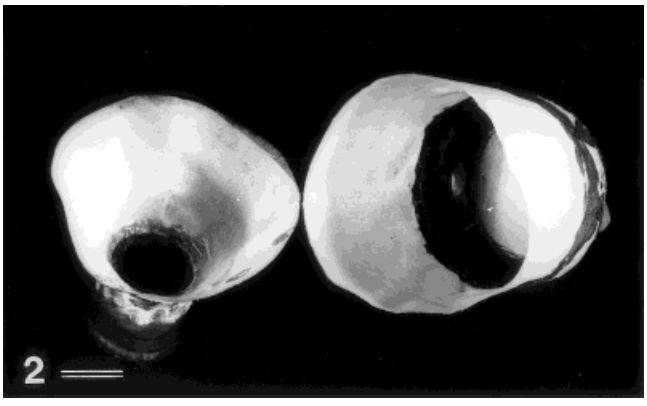

Fig. 2. Baskets for collecting specimen droplets are constructed of nylon mesh attached to a polypropylene base with silicone sealer. The bottom of the base is also composed of mesh to allow the cryogen and substitution media to drain. Two different designs used in our lab are pictured. Scale bar = 1 cm.

MATERIALS AND METHODS

Mixed cultures of the naked freshwater dinoflagellate *Gymnodinium acidotum* (15–25 × 20–35 µm) and the cryptomonad, *Chroomonas coerulea* (3 × 8 µm, no.

TABLE 2. Published criteria for good preservation in rapidly-frozen, freeze-substituted cells

Structure	Characteristics	Reference
Nucleus	Nuclear envelope with smooth contour	von Schack and Fakan (1993)[1]
	Pores with electron-dense material	
	Chromatin with homogenous texture	
	Fibrillar and granular material in nucleoplasm	
	Nucleolus with distinct regions	
Ground cytoplasm	Ice-induced spaces less than 30 nm	Bridgman and Reese (1984)
	Dense, granular matrix with filaments	
Mitochondria	Closed peripheral membrane space	Malhotra and Harreveld (1965)
	Open/partially open peripheral membrane space	Dalen et al. (1992b)
	Open intracristal space	
	Smooth outer contour	
Golgi apparatus	Electron-dense particles on membranes	Ueda and Noguchi (1986)
	Fibrils located within lumina	
	Dense vesicles associated with cisternae	
	Cisternae have smooth contour	
Chloroplasts	Envelope and thylakoids with good contrast	Sluiman and Lokhorst (1988)
	Smooth outer contour	
Microtubules	Lumen of transverse section is empty and round	Lancelle et al. (1987)
	Often associated with other elements such as microfilaments or ER	
	Occasional cross-bridges to adjacent MT's	
Microfilaments	Occur singly, as loose meshworks or in bundles	Bridgman and Reese (1984)
	Actin and myosin retain good antigenicity	Lancelle and Hepler (1989)
	Approximately 7 nm in width	Bridgman and Dailey (1989)

[1]Review article.

ChSP-PK supplied by P. Kugrens, Colorado State University, Ft. Collins, CO) were grown according to the protocol of Fields and Rhodes (1991). Cells were grown in 250-ml flasks to log phase at a light intensity of 150 μE m^{-2} s^{-1}, centrifuged at 40*g* for 10 minutes, and resuspended in 2.0 ml of fresh media. *Prochlorococcus marinus* (0.5–1.0 μm) was supplied by S. Chisholm (Massachusetts Institute of Technology, Cambridge, MA), grown to log phase in K/10 (-Cu) media at a light intensity of 100 μE m^{-2} s^{-1}, centrifuged at 800*g* for 20 minutes, and resuspended in 1 ml of fresh media. *Dictyostelium discoideum* amoebae (strain DH1) were grown axenically to a density of 2×10^6 cells ml^{-1} in HL5 medium in 125-ml flasks with constant aeration. Amoebae were concentrated at 500*g*, rinsed once in 17 mM phosphate buffer (pH 6.6), and resuspended in 2 ml of phosphate buffer.

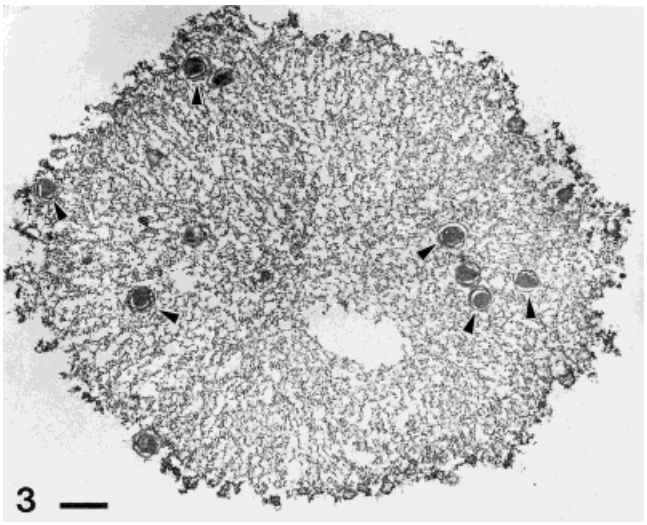

Fig. 3. *Prochlorococcus* cells (arrowheads) entrapped in a matrix of salts that precipitated during freeze substitution. In this case, the size and shape of the precipitates reflects the size and shape of the droplet upon freezing. The apparent flattening of the droplet may be the result of the impact of entry into the cryogen. Formation of these aggregates aided in retaining the small cells in the collection basket and allowed larger mesh sizes to be used in order to facilitate the exchange and drainage of cryogen and substitution media. Scale bar = 1 μm.

Spray-Freezing

The freezing chamber used in this study consists of an aluminum cup (I.D. 40 mm, depth 60 mm) placed within a Styrofoam container (O.D. 105 mm, I.D. 85 mm, depth 85 mm). The Styrofoam container (Fig. 1) is fitted with a clear Plexiglas cover (12-mm thick) with a 40-mm hole in the center through which specimens are sprayed. A hole located at the periphery of the cover allows liquid nitrogen to be added to the outer container through a plastic funnel; a second peripheral hole allows propane to be condensed into the aluminum cup through coiled copper tubing. Liquid nitrogen is used to cool the copper coils (O.D. 5 mm) and liquefy the propane gas, which rapidly condenses in the inner cryochamber as long as sufficient liquid nitrogen is maintained in the outer chamber. Propane influx is monitored using flow meters located between the propane tank and the cryochamber to prevent intermittent bursts of gas and liquid that can splash propane out of the chamber. Approximately 70 ml of propane is collected in the aluminum freezing compartment (see Ryan and Liddicoat, 1987, for precautions in handling propane). Mixing the propane with a magnetic stirring bar in the bottom of the freezing chamber prevented the solidification of the liquid propane during condensation and specimen freezing. The temperature of the liquid propane was measured using a lab-made copper-constantan thermocouple placed just below the surface of the liquid propane. Liquid nitrogen was added manually to the outer chamber as needed in order to maintain the temperature of the propane between 83 and 88 K (−190 and −185°C); propane freezes below 81 K (−192°C).

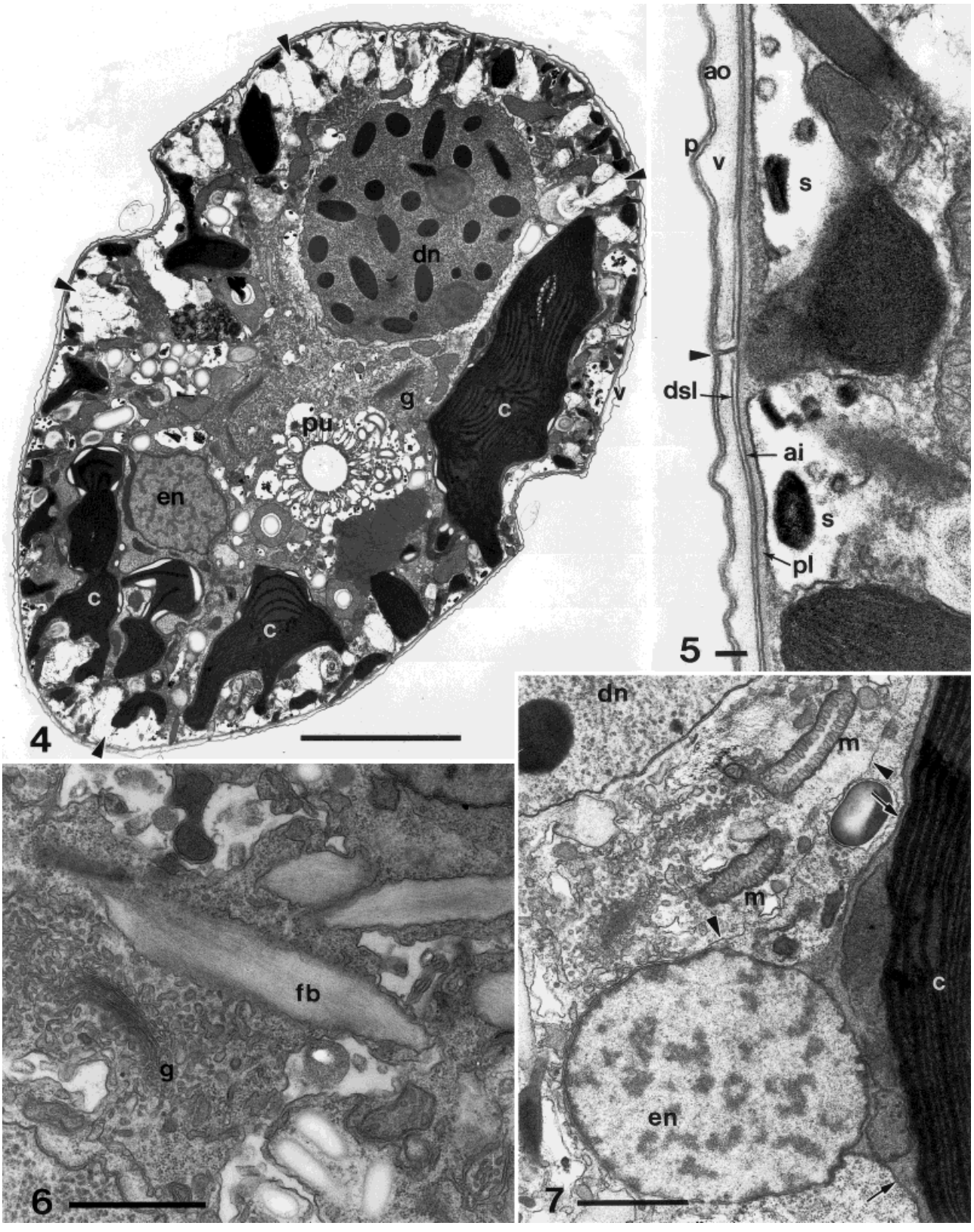

Figs. 4–7.

All cell suspensions were sprayed with a commercially available airbrush (Model HH, Paasche Airbrush Company, Harwood Heights, IL) connected to a nitrogen gas pressure tank. The airbrush was equipped with a needle valve that adjusted the orifice size, thereby regulating the droplet diameter. The optimal pressure and orifice setting were determined experimentally by spraying cells at room temperature onto glass slides and examining them for intactness and motility with a light microscope at a magnification of ×400. The actual droplet size was calculated by spraying water onto a liquid nitrogen-cooled copper block. The resulting spheres of ice were then measured under a thin layer of liquid nitrogen using a stereo dissecting microscope. When the droplet size generated by the airbrush was 50–100 µm and pressures were below 200 kPa (1.5 torr; 29.0 psi), dinoflagellate and cryptomonad cells remained unaltered when sprayed at room temperature, whereas smaller droplet sizes or higher pressures frequently resulted in fragmented or nonmotile dinoflagellates. Since the *Prochlorococcus* cells are less than 1 µm in diameter, the droplet size was adjusted to <20 µm when freezing these cells. For ultrarapid freezing, cells were sprayed at 170 kPa (1.27 torr; 24.7 psi) from a distance of 8–10 cm through the central hole of the Plexiglas cover into the liquid propane. Samples were sprayed in short bursts with 10–15-second intervals to allow recovery of the cryogen temperature. A concentrated cell suspension of 2 ml can be frozen in approximately 40 min.

Spray-frozen cells were collected in a tapered basket (Fig. 2) constructed of a polypropylene base with sides and bottom of 10- or 35-µm nylon mesh (Small Parts, Inc., Miami Lakes, FL) depending on the size of the specimen. Nylon mesh portions of the baskets were fastened with silicone sealer, which is compatible with cryogenic temperatures and is inert in the substitution and post-fixation media. Baskets were made to fit tightly within the freezing chamber and were inserted prior to the addition of liquid propane, which was added until the level was just below the top of the mesh basket. Figure 2 shows two variations in collection basket construction.

Freeze Substitution

Upon completion of freezing, the Plexiglas cover was removed, the nylon mesh basket was lifted and most of the liquid propane drained through the mesh. Propane remaining in the nylon basket was eliminated by transferring the basket through three washes (50 ml each) of distilled acetone at 188 K (−85°C). The large volume of propane remaining in the device was evaporated passively in a fume hood under a stream of dry nitrogen introduced through the hole that was previously used to fill the liquid nitrogen reservoir. The central hole in the Plexiglas was covered with a small plastic Petri dish to reduce condensation of water and oxygen in the chamber.

After rinsing for 30–60 minutes, the nylon basket was transferred to 50 ml of anhydrous acetone containing 1% tannic acid and 1% anhydrous glutaraldehyde at 188 K (−85°C). Freeze substitution was carried out either on dry ice at 195 K (−78°C) with constant agitation for 16–24 hours or in an ultralow freezer at 185 K (−88°C) for 72 hours with occasional agitation. Freeze-substituted cells in the nylon basket were rinsed three times in 50 ml of anhydrous acetone at 188 K (−85°C), then transferred to acetone with 1% OsO_4 at 188 K (−85°C) and warmed slowly to 248 K (−25°C) over 8 hours and then to 277 K (4°C) over 16 hours. After three rinses of acetone at 277 K (4°C), cells were pipetted from the mesh basket to Eppendorf microfuge tubes and either infiltrated with resin or gradually rehydrated over 1 hour with 0.05 M PIPES buffer (pH 7.4) at 277 K (4°C). Rehydrated cells were post-fixed in 1% OsO_4 in 0.05 M PIPES at 277 K (4°C) for 1 hour, rinsed 3 times in buffer, then dehydrated in a graded acetone series at 277 K (4°C).

Cells were infiltrated in either Spurr's resin (Spurr, 1969) or EmBed 812 (Electron Microscopy Sciences, Fort Washington, PA) and polymerized at 343 K (70 K) for 18–24 hours. Silver sections were cut with a diamond knife on a Reichert Ultracut ultramicrotome and stained with the double lead staining method of Daddow (1986) using a modified Sato's lead stain. Sections were viewed using a Zeiss (Thornwood, NY) 10a transmission electron microscope at an accelerating voltage of 80 kV. Cells were examined for ice crystal damage at a magnification of ×25,000. Freezing quality was assessed according to criteria listed in Table 2.

Standard Chemical Fixation

Gymnodinium acidotum cells from log phase cultures were fixed in 2% glutaraldehyde/1% OsO_4 in 0.1 M PIPES buffer (pH 7.8) for 1 hour at room temperature, then post-fixed in 1% OsO_4 in 0.1 M PIPES for 30 minutes. Fixed cells were concentrated in 2% ultralow temperature agarose (United States Biochemical Corp., Cleveland, OH), dehydrated through a graded ethanol series, and embedded in Spurr's resin as above.

Figs. 4–7. Chemical fixation of *Gymnodinium acidotum*. ai, amphiesmal vesicle inner membrane; ao, amphiesmal vesicle outer membrane; c, chloroplast; dsl, dark staining layer; dn, dinophycean nucleus; en, endosymbiont nucleus; g, Golgi body; m, mitochondrion; fb, fibrillar bundle; p, plasma membrane; pl, pellicle; pu, pusule; s, amphisome; v, amphiesmal vesicle.

Fig. 4. Whole cell showing peripheral vacuolization (arrowheads), swelling of the amphiesmal vesicles, and general shrinkage within the cytoplasm. Nuclear membranes exhibit a wrinkled contour and vesicles of the pusule appear collapsed. Scale bar = 5 µm.

Fig. 5. The amphiesma is composed of an external plasma membrane and underlying amphiesmal vesicles. The outer and inner amphiesmal vesicle membranes are connected at sutures (arrowhead). A single membrane, or dark staining layer, lies within each vesicle and does not appear to be connected to any other structure. A pellicle, composed of electron dense material, lies directly beneath the amphiesmal vesicles. Amphiesmal vesicles appear empty and swollen after chemical fixation, and the underlying amphisomes are disrupted. Scale bar = 0.1 µm.

Fig. 6. Cytoplasm of chemically-fixed *G. acidotum* demonstrating excessive vesiculation around the Golgi body. The bundle (fb) in this figure lacks distinct fibrils. Scale bar = 1 µm.

Fig. 7. Portion of cytoplasm showing mitochondria and the endosymbiont. The membrane delimiting the endosymbiont compartment (arrowheads) often appears broken or indistinct. However, the chloroplast endoplasmic reticulum (arrows) surrounding the endosymbiont chloroplast is usually visible. The mitochondria in the dinoflagellate cytoplasm have swollen, tubular cristae when chemically fixed. Scale bar = 1 µm.

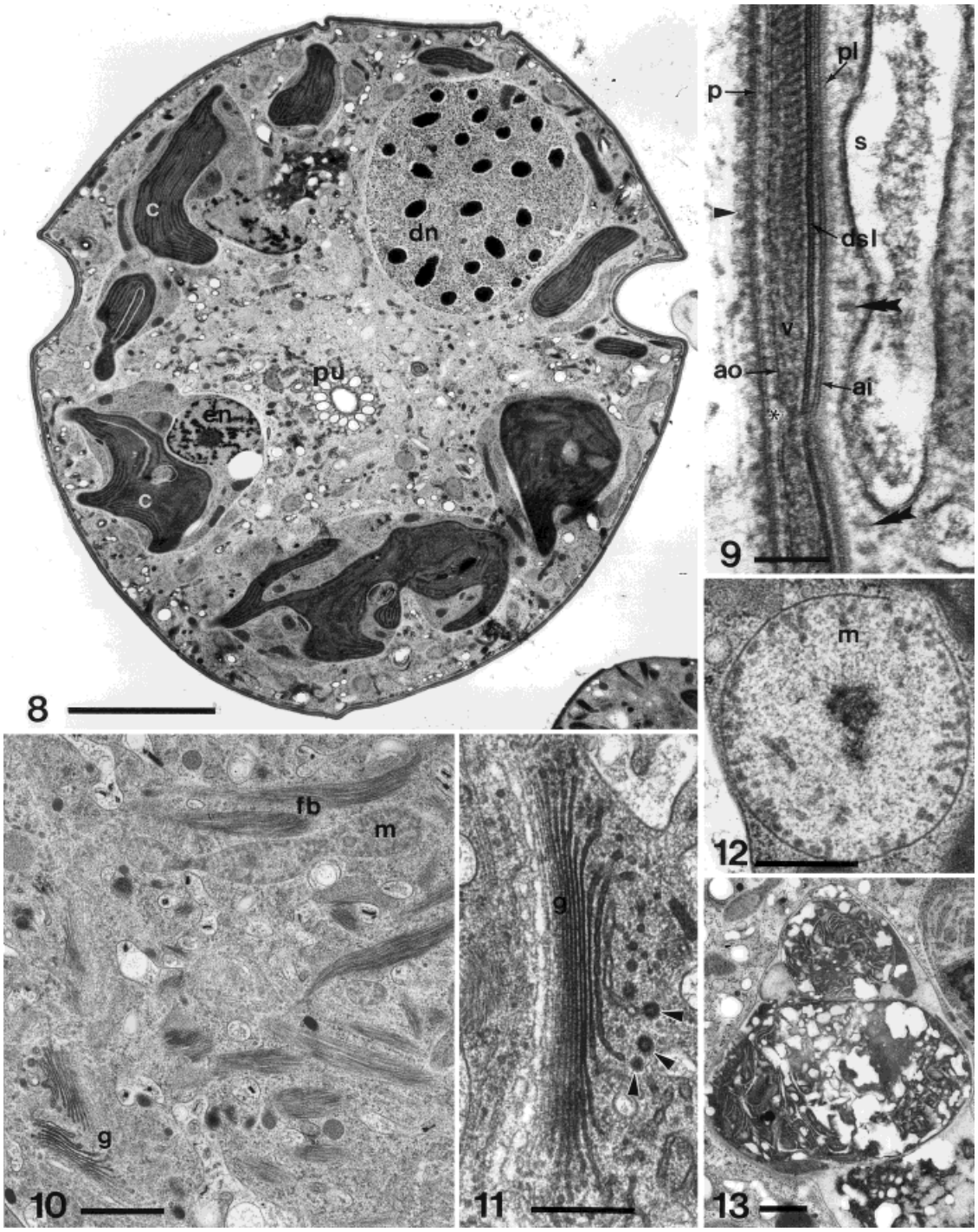

Figs. 8–13. Spray-frozen, freeze-substituted *G. acidotum*. ai, amphiesmal inner membrane; ao, amphiesmal outer membrane; c, chloroplast; dsl, dark staining layer; dn, dinophycean nucleus; en, endosymbiont nucleus; g, Golgi body; m, mitochondrion; fb, fibrillar bundle; p, plasma membrane; pl, pellicle; pu, pusule; s, amphisome; v, amphiesmal vesicle.

Fig. 8. Entire cell demonstrating that boundaries of endosymbiotic compartments are readily distinguishable and that the peripheral cytoplasm is continuous to the cell cortex. Also note the smooth contours of structures such as the dinoflagellate nucleus and pusule, and the absence of disrupted amphisomes at the cell periphery (compare Fig. 4). Scale bar = 5 µm.

Fig. 9. Amphiesma of freeze-substituted dinoflagellates have a distinct glycocalyx (arrowhead) coating the plasma membrane. The electron-dense material filling the amphiesmal vesicle has a periodic substructure and makes the connection between the inner and outer amphiesmal membranes more difficult to resolve at the sutures (*). The dark staining layer and pellicle are distinct and the amphisomes beneath the amphiesma are intact. Obliquely sectioned cortical microtubules (double arrowheads) are also visible between the pellicle and amphisome. Scale bar = 0.1 µm.

Fig. 10. Typical freeze-substituted central cytoplasm of the dinoflagellate. Ground cytoplasm is dense and structures such as the Golgi bodies and mitochondria are distinct and highly ordered. The filamentous nature of the fibrillar bundles is clearly shown. Scale bar = 1 µm.

Fig. 11. Golgi body showing little extraneous vesiculation. Coated vesicles (arrowheads) are present at the forming face of the golgi stack. Scale bar = 0.5 µm.

Fig. 12. Cross-section of typical freeze-substituted mitochondrion. Cristae are more flattened than in chemically-fixed mitochondria; outer and inner mitochondrial membranes are closely appressed. Slight peripheral damage of undetermined origin is visible on the upper right. Scale bar = 0.5 µm.

Fig. 13. Digestive vacuole with well defined bounding membrane. Scale bar = 1 µm.

RESULTS

All cell types, regardless of size, could be successfully processed using mesh baskets throughout the process of freezing and freeze substitution. Transferring the basket from the cryogen to the acetone rinses permitted most of the liquid propane to drain from the basket, although the process was slower for smaller mesh sizes. After the third rinse in acetone, traces of propane gas were no longer apparent in the acetone. Incompletely substituted solutions appeared cloudy and white in the glutaraldehyde/tannic acid/acetone solution due to the presence of ice, whereas dinoflagellate and cryptomonad cultures that were completely freeze-substituted appeared blue-green without any visible trace of ice. Freeze substitution times were reduced from 72 hours to 24 hours when the substitution medium was agitated in the dry ice bath. After warming in the OsO_4/acetone solution, all samples were visible as dark, osmium-stained aggregates. A large proportion of the freeze substituted cells were embedded in a matrix formed by the solutes in the growth medium, which caused cells to be more widely spaced and reduced the number of cells per section (Fig. 3). The extent of the matrix was reduced when freeze-substituted samples were rehydrated, but rehydration did not completely eliminate the matrix. Sectioning was not hindered by the presence of the matrix.

Comparison of Chemically Fixed With Freeze-Substituted Dinoflagellates

Although the general morphology of chemically-fixed *G. acidotum* cells (Fig. 4) resembles that of living cells, there is evidence of extensive cytoplasmic disruption. The adverse effects of chemical fixation are especially evident within the complex cell cortex, or amphiesma. As described by Wilcox and Wedemeyer (1984), the amphiesma of *G. acidotum* is composed of an outer plasma membrane, with underlying amphiesmal vesicles that contain a free-floating membrane, or dark-staining layer, appressed to the inner membrane of the amphiesmal vesicle. Although the amphiesmal vesicles appear swollen and empty, it is clear from an examination of the sutures that the inner and outer vesicle membranes are continuous, thereby forming distinct vesicles. A thin, electron-dense pellicle layer lies directly beneath the amphiesmal vesicles. The region beneath the pellicle is characterized by large amorphous spaces (Fig. 5) that probably represent disrupted amphisomal vesicles described by Bricheux et al. (1992).

The cytoplasm of chemically fixed *G. acidotum* cells is highly aggregated. The golgi bodies are usually vesiculated (Fig. 6), and the nuclear envelope (Figs. 4 and 7) and mitochondrial membranes (Fig. 7) of chemically fixed cells have a wrinkled contour. The peripheral vesicles of the pusule, a purported osmoregulatory organelle, appear to be collapsed (Fig. 4). The cryptophycean endosymbionts of *G. acidotum*, described by Wilcox and Wedemeyer (1984), are delimited by a single membrane, although it is often indistinct or broken with chemical fixation (Fig. 7). Structures found within the cryptophycean endosymbiont include a nucleus, nucleomorph, and chloroplast, which is associated with a pair of membranes called the chloroplast endoplasmic reticulum, or CER (Fig. 7).

Spray-frozen *G. acidotum* cells demonstrate good freezing even to the center of the cell (Fig. 8). An external "fuzzy" layer (Fig. 9), known as the glycocalyx (Klut et al., 1985), coats the outside of the plasma membrane. In contrast to chemically fixed cells, the amphiesmal vesicles of cryofixed cells are filled with an electron-dense material that often demonstrates periodic striations (Fig. 9). The dark-staining layer, or membrane, lies directly beneath this "plate-like" structure. As in chemical fixation, the dark staining layer appears to be free-floating, but the continuity between the inner and outer amphiesmal vesicle membranes is rather indistinct at the sutures of freeze-substituted material. Beneath the pellicle lie intact electron-translucent amphisomes (Bricheux et al., 1992); cortical microtubules are often visible between the pellicle and amphisomes (Fig. 9).

Within the dense, central cytoplasm of freeze substituted dinoflagellates lies the central chamber of the pusule surrounded by turgid peripheral vesicles (Fig. 8). The central portion of the cryofixed cells also contains scattered bundles of microfibrils (Fig. 10), which are not as distinct in the chemically fixed dinoflagellates. The Golgi and ER membrane systems (Figs. 10 and 11) are well defined in spray-frozen material, and nuclei (Fig. 8), mitochondria (Figs. 8, 10, and 12), and vacuoles (Fig. 13) have smooth rather than wrinkled boundaries. The double membranes of cryofixed dinoflagellate mitochondria (Fig. 12) are so closely appressed that they are often indistinguishable, and the cristae appear to be more like flattened sacs (Fig. 12) than the swollen tubules in mitochondria of chemically fixed cells (Fig. 7). The endosymbiont compartments are structurally distinct from the dinoflagellate cytoplasm, even at low magnifications, because of their denser endoplasm. The endosymbiont compartments are entirely enclosed by a single membrane although the membrane itself is variably stained (see below).

Ultrastructure of Freeze-Substituted *Chroomonas coerulea*

The biflagellated *C. coerulea* cells are generally 8–10 μm in length with flagella originating from a gullet at the anterior end of the cell (Fig. 14). Components of the flagellar apparatus such as microtubules and attachment fibers are well preserved, as are the flagella themselves (Fig. 15). The serrated appearance of the periplast of spray-frozen *C. coerulea* cells (Fig. 14) results from the presence of thin proteinaceous plates. There is no evidence of cytoplasmic shrinkage beneath the periplast in frozen preparations, and the prominent Golgi body exhibits relatively few associated vesicles (Fig. 14). The paired thylakoids of the chloroplast have electron-dense lumina, characteristic for cryptomonads, and pairs of thylakoids are separated by the cytoplasmic face of the unit membranes (Fig. 16). The chloroplast endoplasmic reticulum (CER) is sometimes not immediately apparent because of the density of the cytoplasm, but the compartment bound by the CER, known as the periplastidal space, can be easily located because of differences in density between it and the cytoplasm (Fig. 17). The nucleus has a smooth contour and distinct regions of chromatin (Fig. 14), and the mitochondria exhibit flattened cristae and closely appressed inner and outer membranes (Fig. 17).

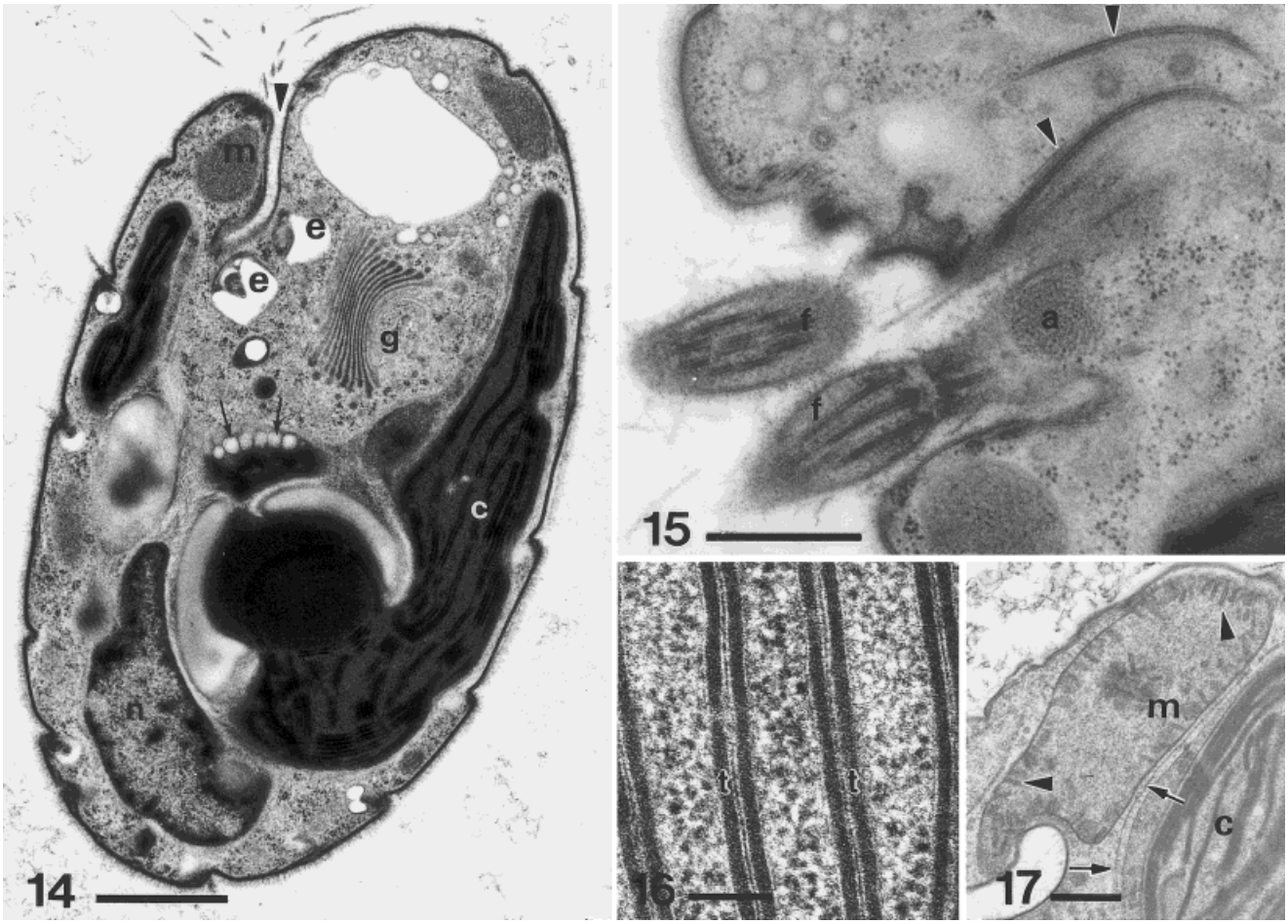

Figs. 14–17. Spray-frozen, freeze substituted cells of the eukaryote, *Chroomonas coerulea*. a, attachment fibers; c, chloroplast; e, ejectosome; f, flagella; g, Golgi apparatus; m, mitochondrion; n, nucleus; t, thylakoid.

Fig. 14. Entire *C. coerulea* cell showing general cellular organization, including a gullet (arrowhead), single chloroplast, posterior nucleus, and centrally located Golgi apparatus. The Golgi are distinct in cryofixed *Chroomonas* cells, and the dense cytoplasm is tightly appressed to the serrated cell wall. Ejectosomes and the stigma (arrows), however, are usually extracted in freeze substituted material. Scale bar = 1 µm.

Fig. 15. Microtubules (arrowheads) and attachment fibers of the cryptomonad flagellar apparatus. The two flagella are also shown near their point of origin. Scale bar = 0.5 µm.

Fig. 16. Paired thylakoids of the *Chroomonas* chloroplast with electron-dense lumina characteristic of cryptomonads. The external portion of the thylakoid unit membrane can be seen between each pair of thylakoids. Scale bar = 0.1 µm.

Fig. 17. Cryptophycean mitochondrion showing close appression of the outer and inner membranes and distinct flattened cristae (arrowheads), which are typical of cryptomonads. The CER (arrows) associated with the chloroplast is also evident. Scale bar = 0.5 µm.

Several potential problems with preservation are also evident in the freeze substituted cryptomonads. The stigma, which is on a stalk emerging from the chloroplast (Fig. 14), has normally been described as an electron-dense group of globules, but in the freeze-substituted material it is electron-translucent, indicating extraction during freeze-substitution. Likewise, the ejectosomes, which occur along the gullet and beneath the periplast, are normally electron-dense after chemical fixation but are electron-translucent in Figure 14.

Ultrastructure of Freeze-Substituted *Prochlorococcus* and *Dictyostelium*

The single, spherical cells of the cyanobacteria, *Prochlorococcus marinus*, are approximately 0.5 µm in diameter. The thylakoids of spray-frozen cells are closely appressed and separated from the cell wall by a region of cytoplasm; the central nucleoid area is distinct (Fig. 18). The most difficult component to visualize in the freeze-substituted *Prochlorococcus* cells was the outer membranes, which were often indistinct, even in freeze-substituted cells that were rehydrated.

The freeze-substituted *Dictyostelium* amoebae (Fig. 19) are bound by a simple plasma membrane that is rather featureless except where pseudopodia arise. The densely staining cytoplasm is rich in ribosomes and endoplasmic reticulum. The membrane-bound lysosomes and mitochondria with closely appressed membranes also have smooth contours, as do the vesicles of the contractile vacuole system. In contrast to the dinoflagellate nucleus, a wide intermembrane space separates the nuclear membranes of *Dictyostelium*. A granu-

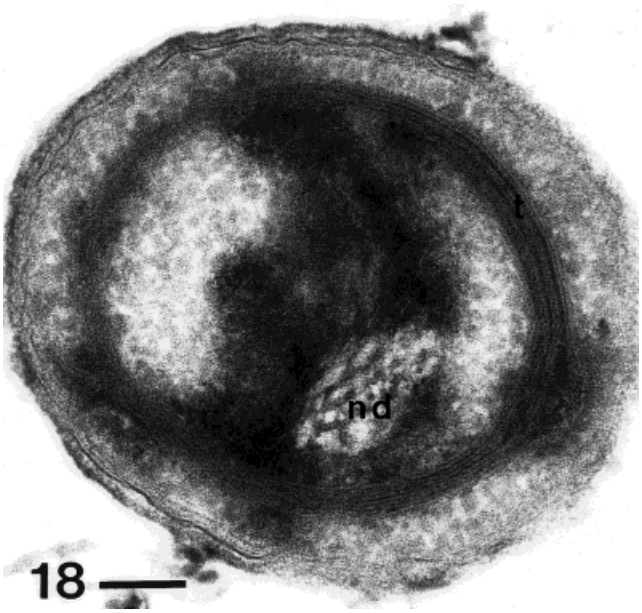

Fig. 18. Entire cell of the cyanobacterium, *Prochlorococcus marinus*, showing nucleoid (nd) and closely appressed thylakoids (t). The multilaminar cell wall is the most difficult component of this cell to preserve, even in rehydrated material. Scale bar = 0.1 μm.

lar material, similar to the nucleoplasm, fills this space and sometimes nuclear pores are filled with electron dense material. The dark-staining nucleoli have distinct regions, including a fibrillar center and granular component. The nucleoplasm is predominantly composed of a homogenous granular material but fibrillar structures are also present.

Effect of Post-Substitution and Infiltration Procedures

Good freezing, as outlined in Table 2, was observed in 71% of the dinoflagellate cell profiles, 86% of the cryptomonad cell profiles, and 95% of the *P. marinus* cells. Nearly all of the dinoflagellate, cryptomonad, and *Prochlorococcus* cells observed at the EM level appeared intact; few cell fragments were observed. A small percentage of the dinoflagellate cells (<5%) had localized areas of sheared amphiesmal vesicles through which cytoplasm was sometimes extruded. A higher proportion of the *Dictyostelium* cells were broken, and many isolated organelles were observed between intact amoebae, but the overall success rate was similar to the dinoflagellate.

The method of processing frozen specimens after substitution had a significant effect on the quality of membrane staining in the dinoflagellates. Substituted cells that were immediately infiltrated and embedded in Spurr's resin often had negatively stained or poorly preserved membranes, particularly in the nuclear envelopes and the boundary membrane of the endosymbiont (Fig. 20). Shrinkage around the dinophycean nucleus and chromosomes, as well as chromosomal extraction, was commonly observed in Spurr's-embedded material (Fig. 8). Infiltration and polymerization in Epon resin following freeze substitution resulted in improved membrane preservation and less extraction of chromosomes although holes were still common at the periphery of chromosomes (not shown). The outer membrane of the endosymbiont was still inconsistently stained in Epon-embedded material.

When freeze substituted cells were rehydrated and post-fixed in OsO_4, the quality of membrane preservation was improved in material embedded in either Epon or Spurr's resin. In *Gymnodinium*, chromosomes were condensed and free of holes (Fig. 21), the boundary membrane and chloroplast-associated membranes of the endosymbiont were usually positively stained, and nuclear envelopes were consistently stained (Fig. 22).

DISCUSSION

Operation and Effectiveness of Spray-Freezer

Previously described devices for spray- and specimen jet-freezing have had more complicated designs, are more difficult to use, and have yielded inconsistent results (Bachmann and Schmitt, 1971; Gilkey and Staehelin, 1986; Knoll et al., 1991) when compared with the design presented here. The objective of this study was to develop a spray-freezing device with: (1) simplicity and affordability; (2) efficient recovery of cell suspensions for freeze substitution; and (3) a good success rate for high quality freezing of specimens that maintain cellular integrity. We have shown that a spray-freezing apparatus with these properties can be assembled and that this can be fabricated from components easily accessible to most laboratories.

One of the most important design features is the mesh collection basket, which can be constructed to retain various cell sizes and can be made to fit available cryogenic chambers (Fig. 2). Collecting samples in the mesh basket simplifies the task of removing the cryogen. In previous spray-freezing studies, the cryogen has usually been removed under a vacuum at 194 K (−79°C) (Bachmann and Schmitt, 1971), a potentially dangerous step since most cryogens are highly flammable. In this study, the large volume of propane used in freezing presumably contributes to thermal stability and freezing efficiency. Propane was removed relatively quickly and safely by draining the mesh. Residual propane in the basket was removed during subsequent acetone rinses.

Collecting the frozen droplets in baskets makes spray-freezing ideal for freeze substitution because the frozen suspensions can be rapidly transferred to various substitution media at low temperatures. The use of relatively large volumes of acetone for freeze substitution keeps the acetone from reaching water saturation, which is reported to be less than 2% water at 188 K (−85°C) (Hippe-Sanwald, 1993). The greater thermal retention of larger volumes of substitution media and the increased efficiency of moving samples between substitution media may also reduce the likelihood of recrystallization. Although dry ice is near the critical temperature of recrystallization for some cell types (Menco, 1986), the elevated substitution temperature did not appear to affect the freezing quality and probably increased the substitution rate. The temperature of recrystallization, however, is species-specific, so caution should be used in freeze substituting at higher temperatures.

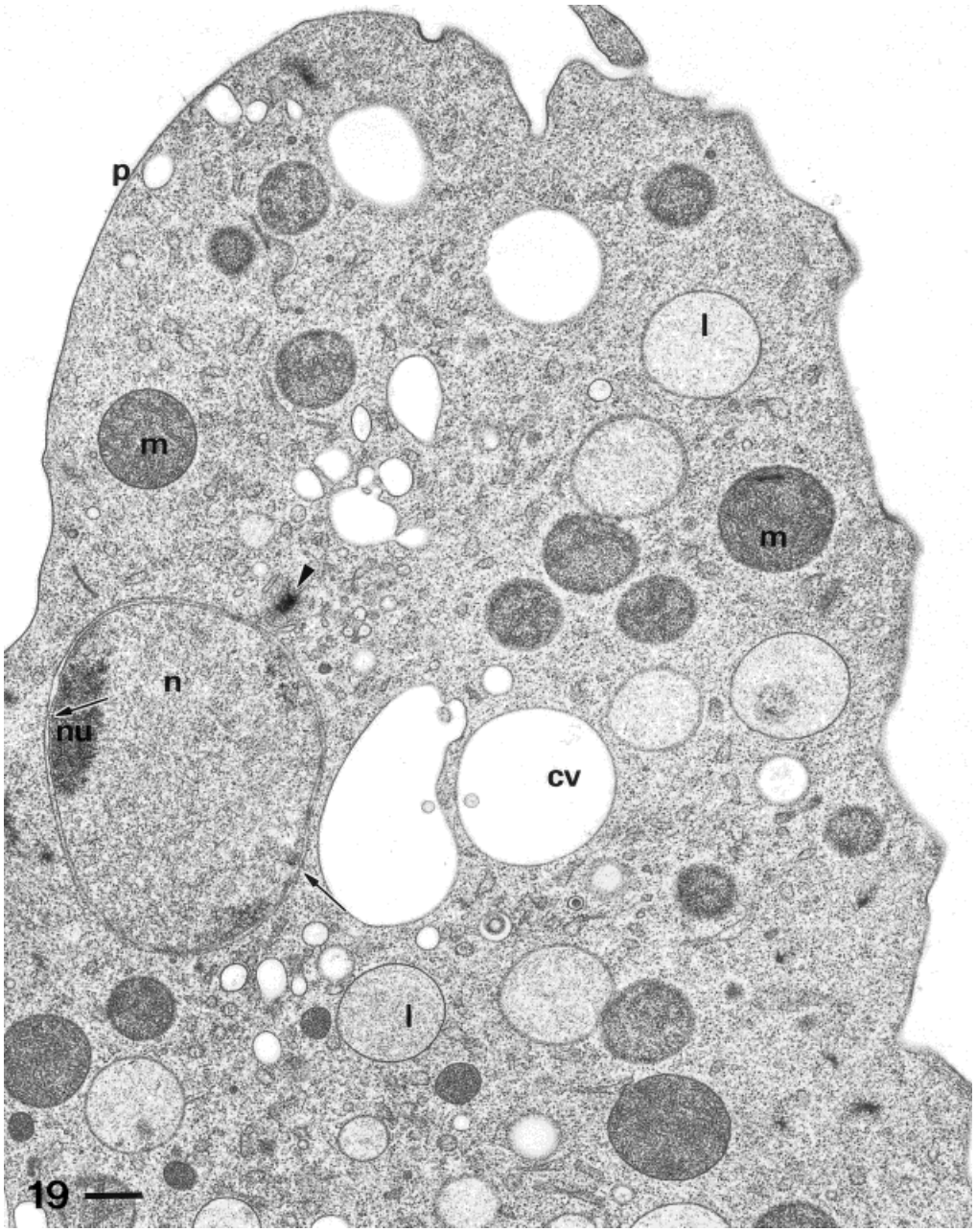

Fig. 19. A portion of a spray-frozen *Dictyostelium discoideum* cell showing the major organelles, including the contractile vacuole system (cv), lysosomes (l), mitochondria (m), and nucleus (n) with a nucleolus (nu). A nucleus associated body (arrowhead), corresponding to a centrosome, is also visible as well as nuclear pores (arrows). There is a wide intermembrane space between the nuclear membranes, but the double membranes of the mitochondria are tightly appressed. The lack of ice crystals and the smooth contours of the organelles and plasma membrane (p) are indications of good freezing. Scale bar = 0.5 µm.

Some authors have suggested that spray-freezing is only suitable for cells on the order of 1–2 µm because of poor freezing in larger cells (Gilkey and Staehelin, 1986). Others have observed shearing of larger cells upon exiting an airbrush (Bachmann and Schmitt-Fumian, 1973; Plattner and Knoll, 1984; Plattner et al., 1973). Neither of these potential problems was evident in the majority of cells examined in this study. The high rate of good freezing in the large dinoflagellates may be attributed to the attention given to obtaining the smallest possible droplet size while maintaining cellular integrity. Measuring the droplets sprayed onto a cold metal surface provided a simple and immediate method of determining the optimum droplet size. Since droplet size was varied with an adjustable aperture on the air brush, as well as through gas pressure, specimen damage may have been minimized. Past spray-freezers have used only changes in gas pressure to reduce sample fragmentation. Most of the fragmented cells in this study were observed in the *Dictyostelium*

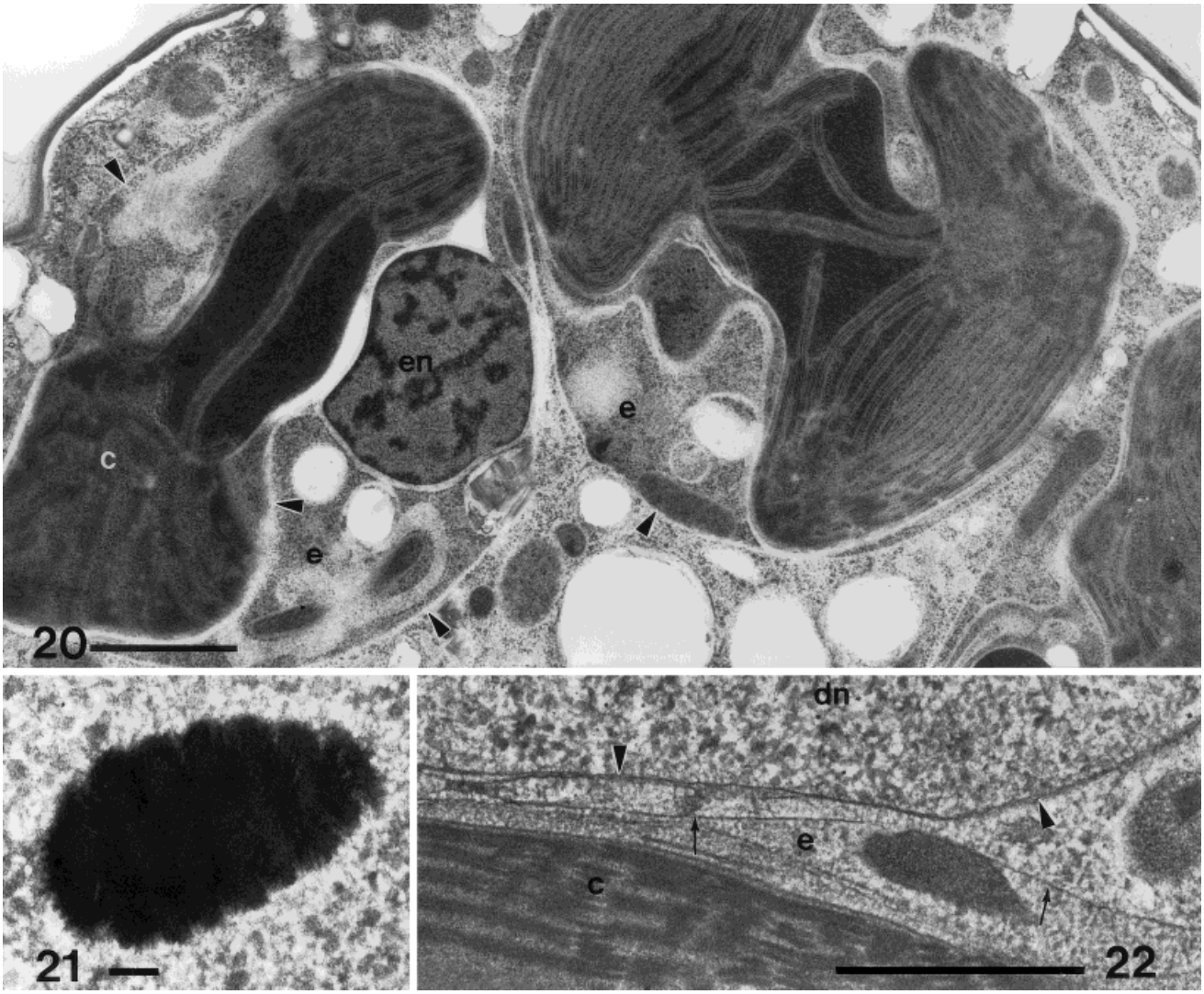

Figs. 20–22. Spray-frozen, freeze-substituted *G. acidotum*. c, chloroplast; dn, dinophycean nucleus; e, endosymbiont; en, endosymbiont nucleus.

Fig. 20. Freeze substituted dinoflagellate infiltrated in Spurr's resin without rehydration. The negative staining of membranes (arrowheads) around and within endosymbiont compartments indicate extraction. Scale bar = 1 μm.

Fig. 21. Condensed chromosome from a freeze-substituted, rehydrated and postfixed cell embedded in Epon resin. Scale bar = 0.1 μm.

Fig. 22. Freeze-substituted, rehydrated and postfixed cell embedded in Spurr's resin. Membranes of the dinoflagellate nucleus (arrowheads) and endosymbiont compartments (arrows) are electron-dense. Scale bar = 1 μm.

sample, possibly because these relatively translucent cells were more difficult to screen for damage at the light microscope level. In contrast, mechanical damage to the large dinoflagellate cells was obvious at the LM level because damaged cells became nonmotile and/or released chloroplasts into the medium. In cell types where damage is not readily apparent, some other form of screening may be employed such as culturing cells sprayed from the airbrush.

Rehydration of Freeze-Substituted Material

A secondary goal of this study was to improve the visibility and preservation of some of the dinoflagellate membranes that appeared to be lost during freeze substitution. The diversity of freeze substitution protocols and recipes in the literature illustrates one of the dilemmas encountered in freeze substitution: various cell types, membranes, and macromolecules respond differently to particular freeze substitution conditions. Standard freeze substitution protocols are adequate for most membranes, but some of the membranes of freeze substituted *G. acidotum* cells were negatively stained. For example, plasma membranes (Fig. 9), Golgi bodies (Figs. 10–11), and digestion vacuole membranes (Fig. 13) were always well preserved and electron dense, but the outer membrane of the endosymbiont compartments and the dinoflagellate nuclear membranes were often negatively stained after conventional freeze substitution (Fig. 20). Some structures like lipid bodies and cryptomonad ejectosomes are typically extracted after freeze substitution (Fig. 14).

Several explanations for poor membrane and lipid preservation during freeze substitution are available. Hess (1990) noted that Spurr's resin extracts freeze-substituted membranes more so than conventionally fixed membranes, and showed that membrane preservation was improved when Epon, rather Spurr's resin, was used after freeze substitution. Similar results for some membrane types were obtained in the current study, but the results were not consistent. The activity and effectiveness of fixatives added to freeze substitution media have also been questionable. Osmium vapors have been reported to begin reacting with lipids at 203 K (−70°C) (White et al., 1976), but the activity of OsO_4 in the presence of a reducer such as acetone at cryogenic temperatures is still unclear. Glutaraldehyde in methanol only crosslinks 20% as much protein at 223 K (−50°C) as at 273 K (0°C) (Humbel and Müller, 1986), raising questions about its effectiveness as a cryofixative at freeze substitution temperatures. Finally, Kellenberger (1991) has pointed out that a hydration shell of tightly bound water around biological membranes and macromolecules may not be adequately removed at freeze substitution temperatures and could inhibit infiltration.

The process of rehydrating the cell, post-fixing in aqueous OsO_4 and dehydrating a second time may expose membranes more effectively to the fixative. Previous investigations demonstrated that rehydration and osmium post-fixation of freeze substituted muscle cells yields improved ultrastructural visualization of membranes without the artifacts of primary chemical fixation (Dalen et al., 1992a,b; Nassar et al., 1986). The current study extends this method to protistan and prokaryotic cells and shows that membrane visibility and morphology are improved as a result of rehydration and postfixation in OsO_4 and that negatively stained membranes were intact and not extracted as suggested by the negative staining.

A secondary advantage of rehydrating freeze substituted material is evident when organic solutes are present in the culture medium. Salts from inorganic media do not hamper sectioning, but organic solutes in some media form crystalline precipitates, which can cause severe knife damage and crumbling of resin blocks (unpublished results). Rehydrating freeze substituted material dissolves these organic precipitates, leaving the reduced osmium that was deposited on the matrix. Rehydrated material from organic media can usually be sectioned without difficulty.

Analysis of Ultrastructural Quality

G. acidotum. One of the most dramatic differences between freeze-substituted and chemically-fixed dinoflagellates is evident at the periphery of *G. acidotum* cells in the amphiesmal and sub-amphiesmal ultrastructure (Figs. 8 and 9). A comparison of Figures 5 and 9 illustrates how chemical preparations that otherwise appear excellent may have structures altered through osmotic effects and extraction. A prominent glycocalyx composed of acid mucopolysaccharides (Klut et al., 1985) coats the surface of the cryofixed amphiesma (Fig. 9), but is often absent on conventionally-fixed amphiesma (Fig. 5). The electron-dense material filling the amphiesmal vesicles is absent in chemically fixed cells, and the pellicle and cortical microtubules are also more prominent after freeze substitution. Conspicuous cortical microtubules below the amphiesma of cryofixed cells (Fig. 9) are difficult to locate in chemically fixed cells as a result of disruption and vacuolization of the amphisomes beneath the cell cortex during preparation. Morrill and Loeblich (1983) suggested that chemical fixation has restricted the localization of microtubules in other dinoflagellate species as well. The interpretation of the dinoflagellate cell cortex has been based upon chemically fixed cells (Morrill and Loeblich, 1983); however, given the drastically different ultrastructural appearance of cryofixed amphiesma, a reinterpretation of amphiesmal structure may be in order. In particular, the significance of the thicker plate-like structures in a "naked" dinoflagellate is unclear, since dinoflagellate taxonomy is based in large part on the presence or absence of thecal plates.

The organelle membranes of chemically fixed dinoflagellates exhibit vesiculation, rearrangements, and wrinkling (Figs. 4–7), which are features typical of glutaraldehyde fixation (Coetzee and van der Merwe, 1985; Fernandez and Staehelin, 1985; Johnson, 1986; Mersey and McCulley, 1978). In contrast, the low water content of Golgi, ER, and mitochondria (Quintana, 1994) contributes to excellent preservation of these organelles by ultrarapid freezing (Figs. 10–12). Closely appressed inner and outer mitochondrial membranes (Fig. 12) are characteristic of freeze-substituted specimens (Malhotra and Harreveld, 1965) and sharply contrast with the spacing observed between the two membranes after chemical fixation (Fig. 7). This feature, along with the swollen cristae characteristic of chemically fixed dinoflagellate mitochondria (Fig. 7), suggests that chemical fixatives also have an osmotic effect on mitochondria.

The filamentous bodies observed in the central cytoplasm of freeze-substituted *G. acidotum* (Fig. 10) are not present in the same form in chemically fixed cells (Fig. 6), suggesting that extraction or chemical modification occurs in these structures during chemical fixation. Previous ultrastructural studies of *G. acidotum* (Farmer and Roberts, 1990a,b; Wilcox and Wedemeyer, 1984) did not identify these structures, but similar bundles, known as cytoplasmic myonemal bundles, have been noted in other dinoflagellates (Cachon et al., 1994). They are thought to be involved in whole cell contractions, although the composition of these bundles is still unclear.

Efforts to determine the true nature of a photosynthetic endosymbiont housed within *G. acidotum* cells have been hampered because of the chemical fixation artifacts mentioned above. In cryofixed *G. acidotum*, the endosymbionts are clearly separated from the dinoflagellate cytoplasm by a single membrane (Fig. 22). Even in endosymbiont compartments where the bounding membrane is poorly preserved or negatively stained, the difference in overall electron-density of the endosymbionts sets them apart from the dinoflagellate cytoplasm (Figs. 8 and 20). In chemically fixed cells, the distinction between dinoflagellate and endosymbiont cytoplasm is often unclear (Figs. 4 and 7), and has contributed to the incorrect suggestion that endosymbiont organelles are directly incorporated in the dinoflagellate cytoplasm (Farmer and Roberts, 1990a).

Other Organisms. The quality and improvement in ultrastructural preservation of cryofixed *C. coerulea*,

D. discoideum, and *P. marinus* cells is similar to that of cryofixed *G. acidotum* cells, with similar success rates. This demonstrates that spray-freezing combined with freeze substitution is applicable to a variety of organisms. Preliminary work with HeLa cells grown in liquid media has also been tried with equal success (Strout, unpublished data), suggesting that SFFS may be applied to non-adherent cells regardless of whether they are protected by a cell wall. We were especially encouraged to find that such a wide range of cell sizes could be processed with the use of the spray-freezer and modified collecting baskets. The superior ultrastructural preservation of cryofixation that has been shown in this investigation and in other studies should be sufficiently compelling to justify the use of ultrarapid freezing. With the development of this spray-freezing technique, routine utilization of freeze substitution for cell suspensions should become readily available to a wide spectrum of cell types, species, applications, and labs.

ACKNOWLEDGMENTS

We thank Dr. Sally Chisholm for supplying *Prochlorococcus marinus*, Dr. Margaret Clarke for *Dictyostelium discoideum* amoebae, and Dr. Paul Kugrens for *Chroomonas coerulea*. This work was supported by a Dissertation Improvement Grant from the National Science Foundation (DEB-9311481), and operating grants from the United States Department of Agriculture (grants 91-37304-6471 and 95-37304-2361).

REFERENCES

Bachmann, L., and Schmitt, W.W. (1971) Improved cryofixation applicable to freeze etching. Proc. Nat. Acad. Sci. U.S.A., 68:2149–2152.

Bachmann, L., and Schmitt-Fumian, W.W. (1973) Spray-freeze-etching of dissolved macromolecules, emulsions and subcellular components. In: Freeze-Etching Techniques and Applications. E.L. Benedetti and P. Favard, eds. Société Française de Microscopie Électronique, Paris, pp. 63–72.

Bachmann, L., Schmitt, W.W., and Plattner, H. (1972) Improved cryofixation demonstrated on freeze-etched solutions, cell fractions and unicellular organisms. In: 5th European Congress for Electron Microscopy, Manchester, UK, pp. 244–245.

Bittermann, A.G., Knoll, G., Nemeth, A., and Plattner, H. (1992) Quantitative immuno-gold labelling and ultrastructural preservation after cryofixation (combined with different freeze-substitution and embedding protocols) and after chemical fixation and cryosectioning. Analysis of the secretory organelle matrix of *Paramecium* trichocysts. Histochemistry, 97:421–429.

Bowers, B., and Maser, M. (1988) Artifacts in fixation for transmission electron microscopy. In: Artifacts in Biological Electron Microscopy. R.F.E. Crang, and K.L. Klomparens, eds. Plenum Press, New York, pp. 13–42.

Bricheux, G., Mahoney, D.G., and Gibbs, S.P. (1992) Development of the pellicle and thecal plates following ecdysis in the dinoflagellate *Glenodinium foliaceum*. Protoplasma, 168:159–171.

Bridgman, P.C., and Dailey, M.E. (1989) The organization of myosin and actin in rapid frozen nerve growth cones. J. Cell Biol., 108:95–109.

Bridgman, P.C., and Reese, T.S. (1984) The structure of cytoplasm in directly frozen cultured cells. I. Filamentous meshworks and the cytoplasmic ground substance. J. Cell Biol., 99:1655–1668.

Cachon, J., Cachon, M., Greuet, C., and Huitorel, P. (1994) Nanofilament dependent motility in dinoflagellates. Biol. Cell, 81:1–10.

Chisholm, S.W., Olsen, R.J., Zettler, E.R., Goericke, R., Waterbury, J.B., and Welschmeyer, N.A. (1988) A novel free-living prochlorophyte abundant in the oceanic euphotic zone. Nature, 334:340–343.

Chisholm, S.W., Frankel, S.L., Goericke, R., Olsen, R.J., Palenik, B., Waterbury, J.B., West-Johnsrud, L., and Zettler, E.R. (1992) *Prochlorococcus marinus* nov. gen. nov. sp.: A marine prokaryote containing divinyl chlorophyll a and b. Arch. Microbiol., 157:297–300.

Coetzee, J., and van der Merwe, C.F. (1985) Penetration rate of glutaraldehyde in various buffers into plant tissue and gelatin gels. J. Microsc., 137:129–136.

Daddow, L.Y.M. (1986) An abbreviated method of the double lead stain technique. J. Submicrosc. Cytol., 18:221–224.

Dalen H., Lieberman, M., LeFurgey, A., Scheie, P., and Sommer, J.R. (1992a) Quick-freezing of cultured cardiac cells in situ with special attention to the mitochondrial ultrastructure. J. Microsc., 168:259–273.

Dalen H., Scheie, P., Nassar, R., High, T., Scherer, B., Taylor, I., Wallace, N.R., and Sommer, J.R. (1992b) Cryopreservation evaluated with mitochondrial and Z line ultrastructure in striated muscle. J. Microsc., 165:239–254.

Dubochet, J., Lepault, J., Freeman, R., Berriman, J.A., and Homo, J.-C. (1982) Electron microscopy of frozen water and aqueous solutions. J. Microsc., 128:219–237.

Farmer, M.A., and Roberts, K.R. (1990a) Comparative analysis of the dinoflagellate flagellar apparatus. IV. *Gymnodinium acidotum*. J. Phycol., 26:122–131.

Farmer, M.A., and Roberts, K.R. (1990b) Organelle loss in the endosymbiont of *Gymnodinium acidotum* (Dinophyceae). Protoplasma, 153:178–185.

Fernandez, D.E., and Staehelin, L.A. (1985) Structural organization of ultrarapidly frozen barley aleurone cells actively involved in protein secretion. Planta, 165:455–468.

Fields, S.D., and Rhodes, R.G. (1991) Ingestion and retention of *Chroomonas* spp. (Cryptophyceae) by *Gymnodinium acidotum* (Dinophyceae). J. Phycol., 27:525–529.

Geanacopoulos, M., and Gear, A.R.L. (1988) Application of spray-freezing to the study of rapid platelet reactions by a quenched-flow approach. Thrombosis Res., 52:599–607.

Gilkey, J.C., and Staehelin, L.A. (1986) Advances in ultrarapid freezing for the preservation of cellular ultrastructure. J. Electron Microsc. Tech., 3:177–210.

Hess, M.W. (1990) Spurr resin affects the ultrastructure of freeze-fixed/freeze substituted pollen grains. Ultramicroscopy, 34:219–221.

Hippe-Sanwald, S. (1993) Impact of freeze substitution on biological electron microscopy. Microsc. Res. Tech., 24:400–422.

Horowitz, R.A., Giannasca, P.J., and Woodcock, C.L. (1990) Ultrastructural preservation of nuclei and chromatin: Improvement with low temperature methods. J. Microsc., 157:205–224.

Humbel, B., and Müller, M. (1986) Freeze substitution and low temperature embedding. In: Science of Biological Specimen Preparation 1995. M. Müller, R.P. Becker, A. Boyde, and J.J. Wolosewick, eds. SEM, Inc., Chicago, pp. 175–183.

Hyde, G.J., Lancelle, S., Hepler, P.K., and Hardham, A.R. (1991) Freeze substitution reveals a new model for sporangial cleavage in *Phytophthora*, a result with implications for cytokinesis in other eukaryotes. J. Cell Sci., 100:735–746.

Johnson, T.J.A. (1986) Glutaraldehyde fixation chemistry: A scheme for rapid crosslinking and evidence for rapid oxygen consumption. In: Science of Biological Specimen Preparation 1985. M. Müller, R.P. Becker, A. Boyde, and J.J. Wolosewick, eds. SEM, Inc., Chicago, pp. 51–62.

Kellenberger, E. (1991) The potential of cryofixation and freeze substitution: Observations and theoretical considerations. J. Microsc., 161:183–203.

Kellenberger, E., Johansen, R., Maeder, M., Bohrmann, B., Stauffer, E., and Villiger, W. (1992) Artifacts and morphological changes during chemical fixation. J. Microsc., 168:181–201.

Klut, M.E., Bisalputra, T., and Antia, N.J. (1985) Some cytochemical studies on the cell surface of *Amphidinium carterae* (Dinophyceae). Protoplasma, 129:93–99.

Knoll, G., Verkleij, A.J., and Plattner, H. (1987) Cryofixation of dynamic processes in cells and organelles. In: Cryotechniques in Biological Electron Microscopy. R.A. Steinbrecht and K. Zierold, eds. Springer-Verlag, Berlin, pp. 258–271.

Knoll, G., Braun, C., and Plattner, H. (1991) Quenched flow analysis of exocytosis in *Paramecium* cells: Time course, changes in membrane structure, and calcium requirements revealed after rapid mixing and rapid freezing of intact cells. J. Cell Biol., 113:1295–1304.

Lancelle, S.A., and Hepler, P.K. (1989) Immunogold labelling of actin on sections of freeze-substituted plant cells. Protoplasma, 150:72–74.

Lancelle, S.A., Callaham, D.A., and Hepler, P.K. (1986) A method for rapid freeze fixation of plant cells. Protoplasma, 131:153–165.

Lancelle, S.A., Cresti, M., and Hepler, P.K. (1987) Ultrastructure of the cytoskeleton in freeze-substituted pollen tubes of *Nicotiana alata*. Protoplasma, 140:141–150.

Lang, R.D.A., and Bronk, J.R. (1978) A study of rapid mitochondrial structural changes in vitro by spray-freezing-etching. J. Cell Biol., 77:134–147.

Lang, R.D.A., Crosby, P., and Robards, A.W. (1976) An inexpensive

spray-freezing unit for preparing specimens for freeze-etching. J. Microsc., 108:101–104.
Lee, M.K.W., McKenzie, R., Kobayashi, K., Garfield, R.E., Forrest, J.B., and Daniel, E.E. (1982) Effects of glutaraldehyde fixative osmolarities on smooth muscle cell volume, and osmotic reactivity of the cells after fixation. J. Microsc., 125:77–88.
Linder, J.C., and Staehelin, L.A. (1979) A novel model for fluid secretion by the trypanosomatid contractile vacuole apparatus. J. Cell Biol., 83:371–382.
Lokhorst, G.M., and Segaar, P.J. (1989) Ultrastructure of zoosporogenesis in the alga *Botridiopsis alpina* (Tribophyceae), as revealed by cryofixation and freeze substitution. Eur. J. Protistol., 24:260–270.
Malhotra, S.K., and Harreveld, A.V. (1965) Some structural features of mitochondria in tissues prepared by freeze-substitution. J. Ultrastruct. Res., 12:473–487.
Mayer, E., and Brüggeller, P. (1982) Vitrification of pure liquid water by high pressure jet freezing. Nature, 298:715–718.
Menco, B.P.M. (1986) A survey of ultra-rapid cryofixation methods with particular emphasis on applications to freeze-fracturing, freeze-etching, and freeze-substitution. J. Electron Microsc. Tech., 4:177–240.
Mersey, B., and McCully, M.E. (1978) Monitoring of the course of fixation of plant cells. J. Microsc., 114:49–76.
Miller, D.C., and Dahl, G.P. (1982) Early events in calcium-induced liposome fusion. Biochim. Biophys. Acta, 689:165–169.
Moor, H. (1973) Cryotechnology for the structural analysis of biological material. In: Freeze-Etching Techniques and Applications. E.L. Benedetti, and P. Favard, eds. Société Française de Microscopie Électronique, Paris, pp. 11–19.
Morrill, L.C., and Loeblich III, A.R. (1983) Ultrastructure of the dinoflagellate amphiesma. Int. Rev. Cytol., 82:151–180.
Murray, J.M., and Ward, R. (1987) Principles for the construction and operation of a device for rapidly freezing suspensions for cryo-electron microscopy. J. Electron Microsc. Tech., 5:279–284.
Nassar, R., Wallace, N.R., Taylor, I., and Sommer, J.R. (1986) The quick-freezing of single intact skeletal muscle fibers at known time intervals following electrical stimulation. Scanning Electron Microsc., 1:309–328.
Pfaller, W., and Rovan, E. (1978) Preparation of resin embedded unicellular organisms without the use of fixatives and dehydration media. J. Microsc., 114:339–351.
Pfaller, W., Rovan, E., and Mairbaurl, H. (1976) A comparison of the ultrastructure of spray-frozen and freeze-etched or freeze-dried bull and boar spermatozoa with that after chemical fixation. J. Reprod. Fertil., 48:285–290.
Plattner, H. (1971) Bull spermatozoa: A re-investigation by freeze-etching using widely different cryofixation procedures. J. Submicr. Cytol., 3:19–32.
Plattner, H., and Bachmann, L. (1982) Cryofixation: A tool in biological ultrastructural research. Int. Rev. Cytol., 79:237–304.
Plattner, H., and Knoll, G. (1984) Cryofixation of biological materials for electron microscopy by the methods of spray-, sandwich-, cryogen-jet-, and sandwich-cryogen-jet-freezing: A comparison of techniques. In: Science of Biological Specimen Preparation for Microscopy and Microanalysis 1983. J.P. Revel, T., Barnard, and G.H. Haggis, eds. SEM, Inc., Chicago, pp. 139–146.
Plattner, H., Fischer, W.M., Schmitt, W.W., and Bachmann, L. (1972) Freeze etching of cells without cryoprotectants. J. Cell Biol., 53:116–126.
Plattner, H., Schmitt-Fumian, W.W., and Bachmann, L. (1973) Cryofixation of single cells by spray-freezing. In: Freeze-Etching Techniques and Applications. E.L. Benedetti and P. Favard, eds. Société Française de Microscopie Électronique, Paris, pp. 81–100.
Quintana, C. (1994) Cryofixation, cryosubstitution, cryoembedding for ultrastructural, immunocytochemical and microanalytical studies. Micron, 25:63–99.
Rand, R.P., Kachar, B., and Reese, T.S. (1985) Dynamic morphology of calcium-induced interactions between phosphatidylserine vesicles. Biophys. J., 47:483–489.
Ridge, R.W. (1990) A simple apparatus and technique for the rapid-freeze and freeze-substitution of single-cell algae. J. Electron Microsc., 39:120–124.
Ryan, K.P. (1992) Cryofixation of tissues for electron microscopy: A review of plunge cooling methods. Scanning Electron Microsc., 6:715–743.
Ryan, K.P., and Knoll, G. (1994) Time-resolved cryofixation methods for the study of dynamic cellular events by electron microscopy: A review. Scanning Electron Microsc., 8:259–288.
Ryan, K.P., and Liddicoat, M.I. (1987) Safety considerations regarding the use of propane and other liquified gases as coolants for rapid freezing purposes. J. Microsc., 147:337–340.
Skaer, H. (1981) Chemical cryoprotection for structural studies. J. Microsc., 125:137–147.
Sluiman, H.J., and Lokhorst, G.M. (1988) The ultrastructure of cellular division (autosporogenesis) in the coccoid green alga, *Trebouxia aggregata*, revealed by rapid freeze fixation and freeze substitution. Protoplasma, 144:149–159.
Spurr, A.R. (1969) A low viscosity epoxy resin embedding medium for electron microscopy. J. Ultrastruct. Res., 26:31–43.
Ueda, K., and Noguchi, T. (1986) Structure of dictyosomes in *Scenedesmus acuminatus* observed by the freeze-substitution method. J. Cell Sci., 82:217–222.
von Schack, M.L., and Fakan, S. (1993) The study of the cell nucleus using cryofixation and cryosubstitution. Micron, 24:507–519.
White, D.L., Andrews, S.B., Faller, J.W., and Barrnett, R.J. (1976) The chemical nature of osmium tetroxide fixation and staining of membranes by X-ray photoelectron spectroscopy. Biochim. Biophys. Acta, 436:577–592.
Wilcox, L.E., and Wedemeyer, G.J. (1984) *Gymnodinium acidotum* Nygaard (Pyrrophyta), a dinoflagellate with an endosymbiotic cryptomonad. J. Phycol., 20:236–242.
Williams, R.C. (1953) A method of freeze-drying for electron microscopy. Exp. Cell Res., 4:188–201.